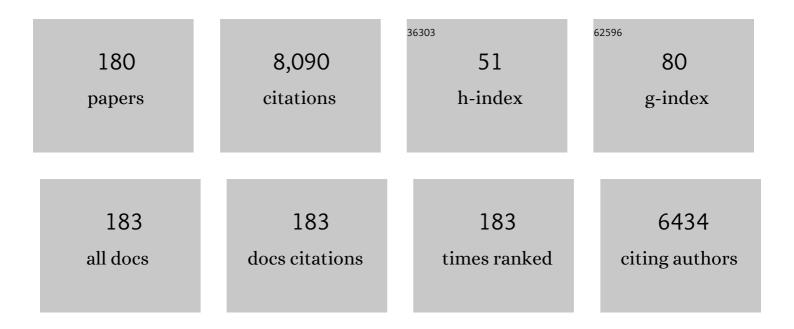
List of Publications by Year in descending order

Source: https://exaly.com/author-pdf/4470214/publications.pdf Version: 2024-02-01



HONCRINCLI

#	Article	IF	CITATIONS
1	Controlled Gas Exfoliation of Boron Nitride into Few‣ayered Nanosheets. Angewandte Chemie - International Edition, 2016, 55, 10766-10770.	13.8	271
2	One-pot extraction combined with metal-free photochemical aerobic oxidative desulfurization in deep eutectic solvent. Green Chemistry, 2015, 17, 2464-2472.	9.0	232
3	Controllable synthesis of Bi ₄ O ₅ Br ₂ ultrathin nanosheets for photocatalytic removal of ciprofloxacin and mechanism insight. Journal of Materials Chemistry A, 2015, 3, 15108-15118.	10.3	202
4	The selectivity for sulfur removal from oils: An insight from conceptual density functional theory. AICHE Journal, 2016, 62, 2087-2100.	3.6	192
5	Few-layered graphene-like boron nitride induced a remarkable adsorption capacity for dibenzothiophene in fuels. Green Chemistry, 2015, 17, 1647-1656.	9.0	167
6	Graphene-Analogue Hexagonal BN Supported with Tungsten-based Ionic Liquid for Oxidative Desulfurization of Fuels. ACS Sustainable Chemistry and Engineering, 2015, 3, 186-194.	6.7	167
7	A state-of-the-art review on dual purpose seaweeds utilization for wastewater treatment and crude bio-oil production. Energy Conversion and Management, 2020, 222, 113253.	9.2	155
8	Adsorption modeling, thermodynamics, and DFT simulation of tetracycline onto mesoporous and high-surface-area NaOH-activated macroalgae carbon. Journal of Hazardous Materials, 2022, 425, 127887.	12.4	155
9	Single-Atom Coated Separator for Robust Lithium–Sulfur Batteries. ACS Applied Materials & Interfaces, 2019, 11, 25147-25154.	8.0	152
10	Boric acid-based ternary deep eutectic solvent for extraction and oxidative desulfurization of diesel fuel. Green Chemistry, 2019, 21, 3074-3080.	9.0	151
11	Tuning the electrophilicity of vanadium-substituted polyoxometalate based ionic liquids for high-efficiency aerobic oxidative desulfurization. Applied Catalysis B: Environmental, 2020, 271, 118936.	20.2	135
12	Taming electronic properties of boron nitride nanosheets as metal-free catalysts for aerobic oxidative desulfurization of fuels. Green Chemistry, 2018, 20, 4453-4460.	9.0	128
13	Sustainable biomass production under CO2 conditions and effective wet microalgae lipid extraction for biodiesel production. Journal of Cleaner Production, 2020, 247, 119398.	9.3	128
14	Carbon-doped porous boron nitride: metal-free adsorbents for sulfur removal from fuels. Journal of Materials Chemistry A, 2015, 3, 12738-12747.	10.3	126
15	Synergistic effect of dual BrÃ,nsted acidic deep eutectic solvents for oxidative desulfurization of diesel fuel. Chemical Engineering Journal, 2020, 394, 124831.	12.7	123
16	Phosphotungstic Acid Immobilized on Ionic Liquid-Modified SBA-15: Efficient Hydrophobic Heterogeneous Catalyst for Oxidative Desulfurization in Fuel. Industrial & Engineering Chemistry Research, 2014, 53, 19895-19904.	3.7	118
17	Copper nanoparticles advance electron mobility of graphene-like boron nitride for enhanced aerobic oxidative desulfurization. Chemical Engineering Journal, 2016, 301, 123-131.	12.7	115
18	Synthesis of supported SiW12O40-based ionic liquid catalyst induced solvent-free oxidative deep-desulfurization of fuels. Chemical Engineering Journal, 2016, 288, 608-617.	12.7	113

#	Article	IF	CITATIONS
19	Magnetic g-C ₃ N ₄ /NiFe ₂ O ₄ hybrids with enhanced photocatalytic activity. RSC Advances, 2015, 5, 57960-57967.	3.6	110
20	Metal-Oxide-Mediated Subtractive Manufacturing of Two-Dimensional Carbon Nitride for High-Efficiency and High-Yield Photocatalytic H ₂ Evolution. ACS Nano, 2019, 13, 11294-11302.	14.6	109
21	Experimental investigation on pumpkin seed oil methyl ester blend in diesel engine with various injection pressure, injection timing and compression ratio. Fuel, 2020, 264, 116868.	6.4	108
22	Vibrational analysis and formation mechanism of typical deep eutectic solvents: An experimental and theoretical study. Journal of Molecular Graphics and Modelling, 2016, 68, 158-175.	2.4	105
23	Seaweed-derived biochar with multiple active sites as a heterogeneous catalyst for converting macroalgae into acid-free biooil containing abundant ester and sugar substances. Fuel, 2021, 285, 119164.	6.4	100
24	Effect of lipid-free microalgal biomass and waste glycerol on growth and lipid production of Scenedesmus obliquus: Innovative waste recycling for extraordinary lipid production. Bioresource Technology, 2018, 249, 992-999.	9.6	98
25	An in situ photoelectroreduction approach to fabricate Bi/BiOCl heterostructure photocathodes: understanding the role of Bi metal for solar water splitting. Journal of Materials Chemistry A, 2017, 5, 4894-4903.	10.3	96
26	Microalgae harvest influences the energy recovery: A case study on chemical flocculation of Scenedesmus obliquus for biodiesel and crude bio-oil production. Bioresource Technology, 2019, 286, 121371.	9.6	92
27	Engineering a tandem leaching system for the highly selective recycling of valuable metals from spent Li-ion batteries. Green Chemistry, 2021, 23, 2177-2184.	9.0	91
28	Reversible Formation of gâ€C ₃ N ₄ 3D Hydrogels through Ionic Liquid Activation: Gelation Behavior and Roomâ€Temperature Gasâ€Sensing Properties. Advanced Functional Materials, 2017, 27, 1700653.	14.9	90
29	Study on two-step hydrothermal liquefaction of macroalgae for improving bio-oil. Bioresource Technology, 2021, 319, 124176.	9.6	89
30	A DFT Study of the Extractive Desulfurization Mechanism by [BMIM] ⁺ [AlCl ₄] ^{â^'} Ionic Liquid. Journal of Physical Chemistry B, 2015, 119, 5995-6009.	2.6	88
31	Tuning the Chemical Hardness of Boron Nitride Nanosheets by Doping Carbon for Enhanced Adsorption Capacity. ACS Omega, 2017, 2, 5385-5394.	3.5	86
32	Effect of operating conditions on direct liquefaction of low-lipid microalgae in ethanol-water co-solvent for bio-oil production. Energy Conversion and Management, 2017, 141, 155-162.	9.2	86
33	Theoretical evidence of charge transfer interaction between SO ₂ and deep eutectic solvents formed by choline chloride and glycerol. Physical Chemistry Chemical Physics, 2015, 17, 28729-28742.	2.8	80
34	Synthesis of Ionic-Liquid-Based Deep Eutectic Solvents for Extractive Desulfurization of Fuel. Energy & Fuels, 2016, 30, 8164-8170.	5.1	79
35	Non ovalent Interaction of Atomically Dispersed Cu and Zn Pair Sites for Efficient Oxygen Reduction Reaction. Advanced Functional Materials, 2022, 32, .	14.9	79
36	Enhanced Oxygen Activation Achieved by Robust Single Chromium Atom-Derived Catalysts in Aerobic Oxidative Desulfurization. ACS Catalysis, 2022, 12, 8623-8631.	11.2	78

#	Article	IF	CITATIONS
37	Taming Interfacial Oxygen Vacancies of Amphiphilic Tungsten Oxide for Enhanced Catalysis in Oxidative Desulfurization. ACS Sustainable Chemistry and Engineering, 2017, 5, 8930-8938.	6.7	75
38	Synthesis of boron nitride nanosheets with N-defects for efficient tetracycline antibiotics adsorptive removal. Chemical Engineering Journal, 2020, 387, 124138.	12.7	75
39	Synthesis of mesoporous WO ₃ /TiO ₂ catalyst and its excellent catalytic performance for the oxidation of dibenzothiophene. New Journal of Chemistry, 2017, 41, 569-578.	2.8	72
40	Polyoxometalate-Based Poly(ionic liquid) as a Precursor for Superhydrophobic Magnetic Carbon Composite Catalysts toward Aerobic Oxidative Desulfurization. ACS Sustainable Chemistry and Engineering, 2019, 7, 15755-15761.	6.7	72
41	Silver Nanoparticle-Decorated Boron Nitride with Tunable Electronic Properties for Enhancement of Adsorption Performance. ACS Sustainable Chemistry and Engineering, 2018, 6, 4948-4957.	6.7	71
42	Cu Nanoclusters/FeN ₄ Amorphous Composites with Dual Active Sites in N-Doped Graphene for High-Performance Zn–Air Batteries. ACS Applied Materials & Interfaces, 2020, 12, 31340-31350.	8.0	71
43	Facile synthesis of amphiphilic polyoxometalate-based ionic liquid supported silica induced efficient performance in oxidative desulfurization. Journal of Molecular Catalysis A, 2015, 406, 23-30.	4.8	66
44	Oxidative desulfurization of fuels promoted by choline chloride-based deep eutectic solvents. Journal of Molecular Catalysis A, 2016, 424, 261-268.	4.8	63
45	Tailoring Nâ€Terminated Defective Edges of Porous Boron Nitride for Enhanced Aerobic Catalysis. Small, 2017, 13, 1701857.	10.0	60
46	Highly efficient phenothiazine 5,5-dioxide-based hole transport materials for planar perovskite solar cells with a PCE exceeding 20%. Journal of Materials Chemistry A, 2019, 7, 9510-9516.	10.3	60
47	Immobilizing Highly Catalytically Molybdenum Oxide Nanoparticles on Graphene-Analogous BN: Stable Heterogeneous Catalysts with Enhanced Aerobic Oxidative Desulfurization Performance. Industrial & Engineering Chemistry Research, 2019, 58, 863-871.	3.7	60
48	Hierarchical porous boron nitride with boron vacancies for improved adsorption performance to antibiotics. Journal of Colloid and Interface Science, 2021, 584, 154-163.	9.4	60
49	Night illumination using monochromatic light-emitting diodes for enhanced microalgal growth and biodiesel production. Bioresource Technology, 2019, 288, 121514.	9.6	59
50	A comparative study of the extractive desulfurization mechanism by Cu(II) and Zn-based imidazolium ionic liquids. Green Energy and Environment, 2019, 4, 38-48.	8.7	53
51	Magnetic POM-based mesoporous silica for fast oxidation of aromatic sulfur compounds. Fuel, 2017, 209, 545-551.	6.4	52
52	A simple and cost-effective extractive desulfurization process with novel deep eutectic solvents. RSC Advances, 2016, 6, 30345-30352.	3.6	51
53	Co-pyrolysis mechanism of seaweed polysaccharides and cellulose based on macroscopic experiments and molecular simulations. Bioresource Technology, 2017, 228, 305-314.	9.6	51
54	A comparative study on the quality of bio-oil derived from green macroalga Enteromorpha clathrata over metal modified ZSM-5 catalysts. Bioresource Technology, 2018, 256, 446-455.	9.6	49

#	Article	IF	CITATIONS
55	Supported ionic liquid [Bmim]FeCl ₄ /Am TiO ₂ as an efficient catalyst for the catalytic oxidative desulfurization of fuels. RSC Advances, 2015, 5, 43528-43536.	3.6	45
56	Molybdenum-containing dendritic mesoporous silica spheres for fast oxidative desulfurization in fuel. Inorganic Chemistry Frontiers, 2019, 6, 451-458.	6.0	45
57	Study on the co-operative effect of kitchen wastewater for harvest and enhanced pyrolysis of microalgae. Bioresource Technology, 2020, 317, 123983.	9.6	45
58	Cross-linked FeCl3-activated seaweed carbon/MCM-41/alginate hydrogel composite for effective biosorption of bisphenol A plasticizer and basic dye from aqueous solution. Bioresource Technology, 2021, 331, 125046.	9.6	45
59	Controlled Gas Exfoliation of Boron Nitride into Few‣ayered Nanosheets. Angewandte Chemie, 2016, 128, 10924-10928.	2.0	44
60	Study on the interaction effect of seaweed bio-coke and rice husk volatiles during co-pyrolysis. Journal of Analytical and Applied Pyrolysis, 2018, 132, 111-122.	5.5	44
61	Synthesis of MoSe ₂ /Reduced graphene oxide composites with improved tribological properties for oilâ€based additives. Crystal Research and Technology, 2014, 49, 204-211.	1.3	43
62	Co-pyrolysis of macroalgae and lignocellulosic biomass. Journal of Thermal Analysis and Calorimetry, 2019, 136, 2001-2016.	3.6	43
63	Lattice-Refined Transition-Metal Oxides via Ball Milling for Boosted Catalytic Oxidation Performance. ACS Applied Materials & Interfaces, 2019, 11, 36666-36675.	8.0	42
64	O ₂ Activation and Oxidative Dehydrogenation of Propane on Hexagonal Boron Nitride: Mechanism Revisited. Journal of Physical Chemistry C, 2019, 123, 2256-2266.	3.1	42
65	Highly Efficient Phenoxazine Core Unit Based Hole Transport Materials for Hysteresis-Free Perovskite Solar Cells. ACS Applied Materials & Interfaces, 2018, 10, 36608-36614.	8.0	41
66	One-pot extraction and aerobic oxidative desulfurization with highly dispersed V ₂ O ₅ /SBA-15 catalyst in ionic liquids. RSC Advances, 2017, 7, 39383-39390.	3.6	40
67	TG–FTIR–MS analysis of the pyrolysis of blended seaweed and rice husk. Journal of Thermal Analysis and Calorimetry, 2016, 126, 1689-1702.	3.6	39
68	Few‣ayer Boron Nitride with Engineered Nitrogen Vacancies for Promoting Conversion of Polysulfide as a Cathode Matrix for Lithium–Sulfur Batteries. Chemistry - A European Journal, 2019, 25, 8112-8117.	3.3	39
69	Dual-active-sites design of CoNx anchored on zinc-coordinated nitrogen-codoped porous carbon with efficient oxygen catalysis for high-stable rechargeable zinc-air batteries. Chemical Engineering Journal, 2021, 408, 127321.	12.7	39
70	Co-cultivation of Streptomyces and microalgal cells as an efficient system for biodiesel production and bioflocculation formation. Bioresource Technology, 2021, 332, 125118.	9.6	39
71	lonic liquid-supported 3DOM silica for efficient heterogeneous oxidative desulfurization. Inorganic Chemistry Frontiers, 2018, 5, 2478-2485.	6.0	38
72	Tuning electronic properties of boron nitride nanoplate via doping carbon for enhanced adsorptive performance. Journal of Colloid and Interface Science, 2017, 508, 121-128.	9.4	37

#	Article	IF	CITATIONS
73	Accurate engineering of hexagonal hollow carbon nitride with carbon vacancies: enhanced photocatalytic H ₂ evolution and its mechanism. Journal of Materials Chemistry A, 2021, 9, 20664-20675.	10.3	37
74	Changes in Biochar Functional Groups and Its Reactivity after Volatile–Char Interactions during Biomass Pyrolysis. Energy & Fuels, 2020, 34, 14291-14299.	5.1	36
75	One-Pot Extraction and Oxidative Desulfurization of Fuels with Molecular Oxygen in Low-Cost Metal-Based Ionic Liquids. Energy & Fuels, 2017, 31, 1376-1382.	5.1	35
76	Mechanism research on the pyrolysis of seaweed polysaccharides by Py-GC/MS and subsequent density functional theory studies. Journal of Analytical and Applied Pyrolysis, 2017, 126, 118-131.	5.5	35
77	Synthesis of WO3/mesoporous ZrO2 catalyst as a high-efficiency catalyst for catalytic oxidation of dibenzothiophene in diesel. Journal of Materials Science, 2018, 53, 15927-15938.	3.7	35
78	Theoretical investigation of the interaction between aromatic sulfur compounds and [BMIM]+[FeCl4]â^' ionic liquid in desulfurization: A novel charge transfer mechanism. Journal of Molecular Graphics and Modelling, 2015, 59, 40-49.	2.4	34
79	Designing multifunctional SO ₃ H-based polyoxometalate catalysts for oxidative desulfurization in acid deep eutectic solvents. RSC Advances, 2017, 7, 55318-55325.	3.6	33
80	Co-pyrolysis and catalytic co-pyrolysis of Enteromorpha clathrata and rice husk. Journal of Thermal Analysis and Calorimetry, 2019, 135, 2613-2623.	3.6	33
81	Extractive desulfurization of diesel fuel by amide-based type IV deep eutectic solvents. Journal of Molecular Liquids, 2021, 338, 116620.	4.9	33
82	Preparation of magnetic Ag/AgCl/CoFe ₂ O ₄ composites with high photocatalytic and antibacterial ability. RSC Advances, 2015, 5, 41475-41483.	3.6	32
83	Cyclic Compound Formation Mechanisms during Pyrolysis of Typical Aliphatic Acidic Amino Acids. ACS Sustainable Chemistry and Engineering, 2020, 8, 16968-16978.	6.7	32
84	Mesoporous silica anchored on reduced graphene oxide nanocomposite as anode for superior lithium-ion capacitor. Rare Metals, 2022, 41, 368-377.	7.1	32
85	Tailoring Electronic Properties of Porphyrin Manganese on Boron Nitride for Enhancing Aerobic Oxidative Desulfurization at Room Temperature. ACS Sustainable Chemistry and Engineering, 2020, 8, 1015-1022.	6.7	30
86	Atomic-Layered α-V ₂ O ₅ Nanosheets Obtained via Fast Gas-Driven Exfoliation for Superior Aerobic Oxidative Desulfurization. Energy & Fuels, 2020, 34, 2612-2616.	5.1	30
87	Catalytic co-pyrolysis of seaweeds and cellulose using mixed ZSM-5 and MCM-41 for enhanced crude bio-oil production. Journal of Thermal Analysis and Calorimetry, 2021, 143, 827-842.	3.6	30
88	Efficient fixation of CO2 into carbonates by tertiary N-functionalized poly(ionic liquids): Experimental-theoretical investigation. Journal of CO2 Utilization, 2021, 44, 101427.	6.8	30
89	Fabrication and characterization of tungsten-containing mesoporous silica for heterogeneous oxidative desulfurization. Chinese Journal of Catalysis, 2016, 37, 971-978.	14.0	29
90	Superparamagnetic Mo-containing core-shell microspheres for catalytic oxidative desulfurization of fuel. Colloids and Surfaces A: Physicochemical and Engineering Aspects, 2018, 537, 243-249.	4.7	29

#	Article	IF	CITATIONS
91	One-Pot Multiple-Step Integration Strategy for Efficient Fixation of CO ₂ into Chain Carbonates by Azolide Anions Poly(ionic liquid)s. ACS Sustainable Chemistry and Engineering, 2021, 9, 7074-7085.	6.7	29
92	Novel visible-light-driven Fe ₂ O ₃ /Ag ₃ VO ₄ composite with enhanced photocatalytic activity toward organic pollutants degradation. RSC Advances, 2016, 6, 3600-3607.	3.6	28
93	Boron and Nitride Dual vacancies on Metalâ€Free Oxygen Doping Boron Nitride as Initiating Sites for Deep Aerobic Oxidative Desulfurization. ChemCatChem, 2020, 12, 1734-1742.	3.7	28
94	Advanced Overlap Adsorption Model of Few-Layer Boron Nitride for Aromatic Organic Pollutants. Industrial & Engineering Chemistry Research, 2018, 57, 4045-4051.	3.7	26
95	Ammonium Nitrate-Assisted Synthesis of Nitrogen/Sulfur-Codoped Hierarchically Porous Carbons Derived from Ginkgo Leaf for Supercapacitors. ACS Omega, 2019, 4, 5904-5914.	3.5	26
96	The mechanism of thiophene oxidation on metal-free two-dimensional hexagonal boron nitride. Physical Chemistry Chemical Physics, 2019, 21, 21867-21874.	2.8	26
97	Facile fabrication of molybdenum-containing ordered mesoporous silica induced deep desulfurization in fuel. Colloids and Surfaces A: Physicochemical and Engineering Aspects, 2016, 504, 174-181.	4.7	25
98	An accurate empirical method to predict the adsorption strength for π-orbital contained molecules on two dimensional materials. Journal of Molecular Graphics and Modelling, 2018, 82, 93-100.	2.4	25
99	Experimental investigation of high alcohol low viscous renewable fuel in DI diesel engine. Environmental Science and Pollution Research, 2021, 28, 12026-12040.	5.3	25
100	Hydrogen rich syngas production from sorption enhanced gasification of cellulose in the presence of calcium oxide. Energy, 2021, 228, 120659.	8.8	25
101	Sonochemical assisted fabrication of 3D hierarchical porous carbon for high-performance symmetric supercapacitor. Ultrasonics Sonochemistry, 2019, 58, 104617.	8.2	24
102	Co-pyrolysis of seaweeds with waste plastics: modeling and simulation of effects of co-pyrolysis parameters on yields, and optimization studies for maximum yield of enhanced biofuels. Energy Sources, Part A: Recovery, Utilization and Environmental Effects, 2020, 42, 954-978.	2.3	24
103	Insight into the Mechanism of Glycerol Dehydration and Subsequent Pyridine Synthesis. ACS Sustainable Chemistry and Engineering, 2021, 9, 3095-3103.	6.7	23
104	Insight into the reversible behavior of Lewis–BrÃ,nsted basic poly(ionic liquid)s in one-pot two-step chemical fixation of CO ₂ to linear carbonates. Green Chemistry, 2021, 23, 8571-8580.	9.0	23
105	H2O2 decomposition mechanism and its oxidative desulfurization activity on hexagonal boron nitride monolayer: A density functional theory study. Journal of Molecular Graphics and Modelling, 2018, 84, 166-173.	2.4	22
106	Unraveling the mechanism of CO ₂ capture and separation by porous liquids. RSC Advances, 2020, 10, 42706-42717.	3.6	22
107	Sn-based deep eutectic solvents assisted synthesis of Sn and SnO2 supported hexagonal boron nitrides for adsorptive desulfurization. Chemical Engineering Research and Design, 2019, 144, 11-18.	5.6	21
108	The interaction nature between hollow silica-based porous ionic liquids and CO2: A DFT study. Journal of Molecular Graphics and Modelling, 2020, 100, 107694.	2.4	21

#	Article	IF	CITATIONS
109	Theoretical insights into CO2/N2 selectivity of the porous ionic liquids constructed by ion-dipole interactions. Journal of Molecular Liquids, 2021, 344, 117676.	4.9	21
110	Activation of Nitrogen-Doped Carbon Materials on the C–N Bond and C–O Bond: Modeling Study Toward Enhanced Pyrolysis Products. ACS Sustainable Chemistry and Engineering, 2022, 10, 7473-7484.	6.7	20
111	Adsorption properties of seaweed-based biochar with the greenhouse gases (CO2, CH4, N2O) through density functional theory (DFT). Biomass and Bioenergy, 2022, 163, 106519.	5.7	20
112	One-pot synthesis of ordered mesoporous silica encapsulated polyoxometalate-based ionic liquids induced efficient desulfurization of organosulfur in fuel. RSC Advances, 2015, 5, 76048-76056.	3.6	19
113	Coke formation during rapid quenching of volatile vapors from fast pyrolysis of cellulose. Fuel, 2021, 306, 121658.	6.4	19
114	Amorphous TiO2-supported Keggin-type ionic liquid catalyst catalytic oxidation of dibenzothiophene in diesel. Petroleum Science, 2018, 15, 870-881.	4.9	18
115	A 3D nitrogen-doped graphene aerogel for enhanced visible-light photocatalytic pollutant degradation and hydrogen evolution. RSC Advances, 2020, 10, 12423-12431.	3.6	18
116	Theoretical prediction of the SO2 absorption by hollow silica based porous ionic liquids. Journal of Molecular Graphics and Modelling, 2021, 103, 107788.	2.4	18
117	Efficient and remarkable SO2 capture: A discovery of imidazole-based ternary deep eutectic solvents. Journal of Molecular Liquids, 2021, 330, 115595.	4.9	18
118	Rational Design of Caprolactam-Based Deep Eutectic Solvents for Extractive Desulfurization of Diesel Fuel and Mechanism Study. ACS Sustainable Chemistry and Engineering, 2022, 10, 4551-4560.	6.7	18
119	Impact of yttria stabilized zirconia coating on diesel engine performance and emission characteristics fuelled by lemon grass oil biofuel. Journal of Thermal Analysis and Calorimetry, 2021, 146, 2303-2315.	3.6	17
120	Unraveling the effects of O-doping into h-BN on the adsorptive desulfurization performance by DFT calculations. Journal of Environmental Chemical Engineering, 2021, 9, 106463.	6.7	17
121	First-principles calculations on structural, electronic properties of V-doped 2H-NbSe2. RSC Advances, 2014, 4, 9573.	3.6	16
122	Fluorine‣ubstituted Benzotriazole Core Building Blockâ€Based Highly Efficient Holeâ€Transporting Materials for Mesoporous Perovskite Solar Cells. Solar Rrl, 2020, 4, 1900362.	5.8	16
123	Understanding the Ingenious Dual Role-Playing of CO ₂ in One-Pot Pressure-Swing Synthesis of Linear Carbonate. ACS Sustainable Chemistry and Engineering, 2022, 10, 2556-2568.	6.7	16
124	Hexacyanoferrateâ€based ionic liquids as Fentonâ€like catalysts for deep oxidative desulfurization of fuels. Applied Organometallic Chemistry, 2016, 30, 753-758.	3.5	15
125	Engineering hollow mesoporous silica supported cobalt molybdate catalyst by dissolution-regrowth strategy for efficiently aerobic oxidative desulfurization. Fuel, 2022, 325, 124755.	6.4	15

Study of pyrolytic mechanisms of seaweed based on different components (soluble polysaccharides,) Tj ETQq0 0 0 rgBT /Overlock 10 Tf 14

#	Article	IF	CITATIONS
127	Metal Nanoparticles Confined within an Inorganic–Organic Framework Enable Superior Substrate-Selective Catalysis. ACS Applied Materials & Interfaces, 2020, 12, 42739-42748.	8.0	14
128	Entropy, Entransy and Exergy Analysis of a Dual-Loop Organic Rankine Cycle (DORC) Using Mixture Working Fluids for Engine Waste Heat Recovery. Energies, 2020, 13, 1301.	3.1	13
129	Ammonium Nitrateâ€Assisted Lowâ€Temperature Synthesis of Co, Co ₂ P@CoP Embedded in Biomassâ€Derived Carbons as Efficient Electrocatalysts for Hydrogen and Oxygen Evolution Reaction. ChemistrySelect, 2020, 5, 7338-7346.	1.5	13
130	Engineering Highly Dispersed Pt Species by Defects for Boosting the Reactive Desulfurization Performance. Industrial & amp; Engineering Chemistry Research, 2021, 60, 2828-2837.	3.7	13
131	Multifunctional gold-loaded TiO ₂ thin film: photocatalyst and recyclable SERS substrate. Canadian Journal of Chemistry, 2013, 91, 1112-1116.	1.1	12
132	First-principles study of atomic structure and electronic properties of Si and F doped anatase TiO ₂ . Materials Science-Poland, 2015, 33, 549-554.	1.0	12
133	Influence of torrefaction pretreatment on the pyrolysis characteristics of seaweed biomass. Cellulose, 2019, 26, 8475-8487.	4.9	12
134	Effect of cosolvent and addition of catalyst (HZSMâ€5) on hydrothermal liquefaction of macroalgae. International Journal of Energy Research, 2019, 43, 8841.	4.5	12
135	Catalytic coâ€pyrolysis of macroalgal components with lignocellulosic biomass for enhanced biofuels and highâ€valued chemicals. International Journal of Energy Research, 2022, 46, 2674-2697.	4.5	12
136	Thermal decomposition mechanism of emulsion explosives with phosphatide. Journal of Thermal Analysis and Calorimetry, 2016, 124, 1053-1062.	3.6	11
137	Theoretical prediction of F-doped hexagonal boron nitride: A promising strategy to enhance the capacity of adsorptive desulfurization. Journal of Molecular Graphics and Modelling, 2020, 101, 107715.	2.4	11
138	Enhancement on the tribological properties of poly(phthalazinone ether sulfone ketone) by carbon nanotubeâ€supported graphitic carbon nitride hybrid. Polymer Composites, 2020, 41, 3768-3777.	4.6	11
139	3D Bimodal Porous Amorphous Carbon with Self-Similar Porosity by Low-Temperature Sequential Chemical Dealloying. Chemistry of Materials, 2021, 33, 1013-1021.	6.7	11
140	Engineering Dual Oxygen Simultaneously Modified Boron Nitride for Boosting Adsorptive Desulfurization of Fuel. Engineering, 2022, 14, 86-93.	6.7	11
141	Ag Atom Anchored on Defective Hexagonal Boron Nitride Nanosheets As Single Atom Adsorbents for Enhanced Adsorptive Desulfurization via S-Ag Bonds. Nanomaterials, 2022, 12, 2046.	4.1	11
142	First-principles study of negative thermal expansion mechanism in A-site-ordered perovskite SrCu ₃ Fe ₄ O ₁₂ . RSC Advances, 2015, 5, 1801-1807.	3.6	10
143	Preparation of silver/silver bromide/titanium dioxide/graphene oxide nanocomposite for photocatalytic degradation of 4-chlorophenol. Nanomaterials and Nanotechnology, 2017, 7, 184798041772404.	3.0	10
144	Polyoxometalate-based silica-supported ionic liquids for heterogeneous oxidative desulfurization in fuels. Petroleum Science, 2018, 15, 882-889.	4.9	10

#	Article	IF	CITATIONS
145	Oneâ€step preparation of carbon <scp>fiberâ€ZrO₂</scp> hybrid and its enhancement on the wearâ€resistant properties of polyimide. Polymer Composites, 2021, 42, 2598-2607.	4.6	10
146	Study on the pyrolysis mechanism of unsaturated fatty acid: A combined density functional theory and experimental study. International Journal of Energy Research, 2022, 46, 2029-2040.	4.5	10
147	Atomic structures and electronic properties of Ta-doped 2H-NbSe2. RSC Advances, 2014, 4, 57541-57546.	3.6	9
148	Comparative study of halogen-doped (X Cl, Br, I) hexagonal boron nitride: A promising strategy to enhance the capacity of adsorptive desulfurization. Journal of Environmental Chemical Engineering, 2021, 9, 105886.	6.7	9
149	Fiber hybrid polyimideâ€based composites reinforced with carbon fiber and polyâ€∢i>pâ€phenylene benzobisthiazole fiber: Tribological behaviors under sea water lubrication. Polymer Composites, 2016, 37, 1650-1658.	4.6	8
150	Synthesis of task-specific ternary deep eutectic solvents for deep desulfurization via reactive extraction. Chemical Engineering and Processing: Process Intensification, 2022, 171, 108754.	3.6	8
151	Entropy and Entransy Dissipation Analysis of a Basic Organic Rankine Cycles (ORCs) to Recover Low-Grade Waste Heat Using Mixture Working Fluids. Entropy, 2018, 20, 818.	2.2	7
152	Rational design of the carbon doping of hexagonal boron nitride for oxygen activation and oxidative desulfurization. Physical Chemistry Chemical Physics, 2020, 22, 24310-24319.	2.8	7
153	Ferrimagnetic semiconductor with a direct bandgap. Applied Physics Letters, 2020, 116, .	3.3	7
154	Construction of <scp>2D</scp> / <scp>2D</scp> graphene oxide/ <scp>gâ€C₃N₄</scp> hybrid for enhancing the friction and wear performance of p <scp>oly (phthalazinone ether sulfone ketone)</scp> . Polymer Composites, 2022, 43, 2055-2063.	4.6	7
155	Highly efficient adsorption of Bisphenol A using NaHCO3/CO2 activated carbon composite derived from shrimp shell@cellulose. Environmental Science and Pollution Research, 2022, 29, 68724-68734.	5.3	7
156	Porous liquids for gas capture, separation, and conversion: Narrowing the knowing-doing gap. Separation and Purification Technology, 2022, 297, 121456.	7.9	7
157	Fabrication of dual-mesoporous silica by triblock copolymers and metal-based ionic liquid: efficient and durable catalyst for oxidative desulfurization in fuel. RSC Advances, 2015, 5, 104322-104329.	3.6	5
158	Research on the influence of alkyl ammonium bromides on the properties of Ag/AgBr/GO composites. New Journal of Chemistry, 2016, 40, 1323-1329.	2.8	5
159	Comparative Study of Combustion Properties of Two Seaweeds in a Batch Fluidized Bed. Combustion Science and Technology, 2018, 190, 755-769.	2.3	5
160	SBA-15 supported molybdenum oxide towards efficient catalytic oxidative desulfurization: effect of catalysts. Journal of the Chinese Advanced Materials Society, 2018, 6, 44-54.	0.7	5
161	Unraveling the effect of B-site antisite defects on the electronic and magnetic properties of the quadruple perovskite CaCu ₃ Fe ₂ Nb ₂ O ₁₂ . Physical Chemistry Chemical Physics, 2019, 21, 3059-3065.	2.8	5
162	Transformation of Nitrogen during Microalgae Liquefaction in Subcritical/Supercritical Ethanol. Energy & Fuels, 2020, 34, 14182-14189.	5.1	5

#	Article	IF	CITATIONS
163	Study on Pore Structure of Seaweed Particles After Combustion. Journal of Energy Resources Technology, Transactions of the ASME, 2016, 138, .	2.3	4
164	Rational design of the nonlinear optical materials dinaphtho[2,3-b:2′,3′-d]thiophene-5,7,12,13-tetraone (DNTTRA) and its phenyldiazenyl derivatives using first-principles calculations. Journal of Computational Electronics, 2019, 18, 6-15.	2.5	4
165	Defect Engineering on Boron Nitride for O ₂ Activation and Subsequent Oxidative Desulfurization. ChemPhysChem, 2021, 22, 168-177.	2.1	4
166	Biocrude Production from Hydrothermal Liquefaction of Chlorella: Thermodynamic Modelling and Reactor Design. Energies, 2021, 14, 6602.	3.1	4
167	Synthesis of asymmetric [bis(imidazolyl)-BH ₂] ⁺ -cation-based ionic liquids as potential rocket fuels. RSC Advances, 2021, 11, 38040-38046.	3.6	4
168	Nitrogen transfer mechanism research on the co- pyrolysis macroalgae with polyethylene. Sustainable Energy Technologies and Assessments, 2022, 51, 101886.	2.7	4
169	Thin films of α-Fe2O3 nanoparticles using as nonmetallic SERS-active nanosensors for submicromolar detection. Frontiers of Chemistry in China: Selected Publications From Chinese Universities, 2011, 6, 206-212.	0.4	3
170	Controllable synthesis of graphene oxide–silver (gold) nanocomposites and their size-dependencies. RSC Advances, 2016, 6, 70468-70473.	3.6	3
171	Benzo[1,2- <i>c</i> :4,5- <i>c</i> ′]dithiophene-4,8-dione (BDD) Core Building Block Based Dopant-Free Hole-Transport Materials for Efficient and Stable Perovskite Solar Cell. ACS Applied Energy Materials, 2020, 3, 10333-10339.	5.1	3
172	The electronic structure and physicochemical property of boron nitridene. Journal of Molecular Graphics and Modelling, 2020, 94, 107475.	2.4	2
173	Pyrolysis behaviors of rapeseed meal: products distribution and properties. Biomass Conversion and Biorefinery, 0, , 1.	4.6	2
174	Synthesis and characterization of hypergolic salts based on bis(1H-1,2,3-triazole-1-yl) dihydroborate anion. Journal of Molecular Structure, 2022, 1261, 132850.	3.6	2
175	Hydrogels: Reversible Formation of g ₃ N ₄ 3D Hydrogels through Ionic Liquid Activation: Gelation Behavior and Roomâ€Temperature Gasâ€Sensing Properties (Adv. Funct. Mater.) Tj ETQq1 I	l 0 <i>1</i> 7 89 31	4 rgBT /Overl
176	A half-metallic ferrimagnet of CeCu3Cr4O12 with 4f itinerant electron. Applied Physics Letters, 2020, 117, 132404.	3.3	1
177	Preparation of Biscuit-Like SO2â^'4/ZrO2 Catalyst for Alkylation of o-Xylene with Styrene. Journal of Nanoscience and Nanotechnology, 2020, 20, 3496-3503.	0.9	1
178	Ionic Liquids for Extractive Desulfurization of Fuels. , 2021, , 1-6.		0
179	Facile Construction of Magnetic Ionic Liquid Supported Silica for Aerobic Oxidative Desulfurization in Fuel. Catalysts, 2021, 11, 1496.	3.5	0
180	Preparation of the 1-Methylimidazole Borane/Tetrazole System for Hypergolic Fuels. Molecules, 2022, 27, 4466.	3.8	0